A Journal of the Gesellschaft Deutscher Chemiker

Angewandte International Edition GDCh Chemie

www.angewandte.org

Accepted Article

Title: Confined Pt11+–water clusters in a MOF Catalyze the Low–Temperature Water–Gas Shift Reaction with both CO2 Oxygen Atoms Coming from Water.

Authors: Miguel A. Rivero–Crespo, Marta Mon, Jesús Ferrando–Soria, Christian W. Lopes, Mercedes Boronat, Antonio Leyva–Pérez, Avelino Corma, Juan C. Hernández–Garrido, Miguel López–Haro, Jose J. Calvino, Enrique V. Ramos–Fernandez, Donatella Armentano, and Emilio Pardo

To be cited as: *Angew. Chem. Int. Ed.* 10.1002/anie.201810251
Angew. Chem. 10.1002/ange.201810251

Link to VoR: http://dx.doi.org/10.1002/anie.201810251
http://dx.doi.org/10.1002/ange.201810251

WILEY-VCH

10.1002/anie.201810251

WILEY-VCH

Confined Pt_1^{1+}–Water Clusters in a MOF Catalyze the Low–Temperature Water–Gas Shift Reaction with both CO_2 Oxygen Atoms Coming from Water.

Miguel A. Rivero–Crespo,[a],† Marta Mon,[b],† Jesús Ferrando–Soria,[b] Christian W. Lopes,[a] Mercedes Boronat,[a] Antonio Leyva–Pérez,[a]* Avelino Corma,[a]* Juan C. Hernández–Garrido,[c,d] Miguel López–Haro,[c,d] Jose J. Calvino,[c,d] Enrique V. Ramos–Fernandez,[e] Donatella Armentano[f]* and Emilio Pardo.[b]*

Abstract: The synthesis and reactivity of single metal atoms in low–valence state bound to just water, rather than to organic ligands or surfaces, is a major experimental challenge. Here, we show a gram–scale wet synthesis of Pt_1^{1+} stabilized in a confined space by a well–defined crystallographic first water sphere, and with a second coordination sphere linked to the Metal–Organic Framework (MOF) through electrostatic and H–bonding interactions. The role of the water cluster is not only isolating and stabilizing the Pt atoms, but also regulating the charge of the metal and the adsorption of reactants. This is shown for the low–temperature water–gas shift reaction (WGSR: $CO + H_2O \rightarrow CO_2 + H_2$), where both metal coordinated and H–bonded water molecules trigger a double water attack mechanism to CO and give CO_2 with both oxygen atoms coming from water. The stabilized Pt^{1+} single sites allow performing the WGSR at temperatures as low as 50 ºC.

Metal atoms in low oxidation state barely stabilize with water molecules, since electron back donation is often the major contribution to metal–ligand bonding and water tends to break up before accepting significant electron density in antibonding orbitals. Indeed, it is difficult to find examples of very electron–rich metals just bound to hard donor ligands, where back donation cannot occur. Should water stabilize an electron–rich metal atom, a powerful bifunctional single–atom metal catalyst will be furnished, with external reactants easily activated by electron back donation of the metal site and, at the same time, with Brönsted acid/base mechanisms triggered by the associated water cluster. To achieve this kind of metal species, the use of a supporting solid to accommodate the complex and, concomitantly, keep the water–metal ligation by accepting some electron density, seems a plausible approach.[1]

Metal–Organic Frameworks (MOFs)[2] are crystalline porous materials which present potential wells within their pores to stabilize ultrasmall metal clusters in reduced form, amenable for an atomic level characterization by means of single–crystal X–ray diffraction (SC–XRD).[3] From our point of view, the electrostatic configuration of a suitable MOF structure could also stabilize single metal atoms in low–valence state coordinated to water, where the MOF acts as the final acceptor of electron density, thus preserving water ligation to the metal.

The present manuscript reports the gram–scale synthesis and characterization in depth of a structurally and electronically well–defined Pt_1^{1+} stabilized by water clusters, homogeneously distributed along the channels of an anionic three–dimensional (3D) MOF, with a powerful catalytic activity for the low–temperature water–gas shift reaction (WGSR), a paradigmatic example of reaction easily inhibited by π–acid molecules, i.e. carbon monoxide CO. Experimental and computational results unveil that the Pt_1^{1+} complex catalyzes the WGSR with the participation of at least two surrounding water molecules, to give CO_2 with both oxygen atoms mainly coming from water. Pt^{1+} species are rarely described in the literature and the MOF–supported Pt_1^{1+} constitutes an exceptional case of a single–atom catalyst (SAC) without strong coordinating ligands or surfaces.

Figure 1 shows the crystal structures of three metal–supported MOFs prepared by the solid–state post–synthetic (PS) method[4] and determined by SC–XRD with synchrotron radiation. The very robust and highly crystalline MOF $Ni_2^{2+}\{Ni^{2+}_4[Cu^{2+}_2(Me_3mpba)_2]_3\} \cdot 54H_2O$ (**1**)[5] (Figure 1a) was exchanged with $[Pt(NH_3)]_4^{2+}$ to give the intermediate hybrid material $[Pt^{2+}_2(\mu\text{–}OH_2)(NH_3)_6)]_{0.65}[Pt^{2+}(NH_3)_4]_{0.7}\{Ni^{2+}_4[Cu^{2+}_2(Me_3mpba)_2]_3\} \cdot 65H_2O$ (**2**) (Figure 1b), which was then treated with $NaBH_4$ to yield the final solid material $[Pt^{2+}_2(\mu\text{–}O)(OH)_2(NH_3)_4]_{0.5}Pt_1^{1+}@Na_3\{Ni^{2+}_4[Cu^{2+}_2(Me_3mpba)_2]_3\} \cdot 79H_2O$ (**3**) (Figure 1c, see also Table S1 in Supporting Information).

[a] M. A. Rivero–Crespo, Dr. C. W. Lopes, Dr. M. Boronat, Dr. A. Leyva–Pérez, Prof. A. Corma.
Instituto de Tecnología Química. Universidad Politècnica de València–Consejo Superior de Investigaciones Científicas.
Avda. de los Naranjos s/n, 46022, València, Spain.
E–mails: anleyva@itq.upv.es, acorma@itq.upv.es.

[b] M. Mon, Dr. J. Ferrando–Soria, Dr. E. Pardo.
Departament de Química Inorgànica, Instituto de Ciencia Molecular (ICMol), Universitat de València, 46980 Paterna, València, Spain.
E–mail: emilio.pardo@uv.es.

[c] Dr. J. C. Hernández–Garrido, Dr. M. López–Haro, Prof. J. J. Calvino,
Departamento de Ciencia de los Materiales e Ingeniería Metalúrgica y Química Inorgánica, Facultad de Ciencias, Universidad de Cádiz, Campus Río San Pedro, 11510 Puerto Real, Cádiz, Spain.

[d] Instituto Universitario de Investigación en Microscopía Electrónica y Materiales (IMEYMAT). Facultad de Ciencias. Universidad de Cádiz, Campus Río San Pedro, 11510 Puerto Real, Cádiz, Spain.

[e] Dr. E. V. Ramos–Fernandez.
Laboratorio de Materiales Avanzados, Departamento de Química Inorgánica, Instituto Universitario de Materiales de Alicante, Universidad de Alicante, Apartado 99, Alicante, Spain.

[f] Prof. D. Armentano.
Dipartimento di Chimica e Tecnologie Chimiche, Università della Calabria, 87030 Rende, Cosenza, Italy.
E–mail: donatella.armentano@unical.it.

† These two authors have equally contributed to this work.

Supporting information for this article is given via a link at the end of the document, and includes a PDF file with the experimental section, Figures S1–S27 and Tables S1–S7. Crystallographic data that support the findings of this study have been deposited in The Cambridge Crystallographic Data Centre free of charge, with accession codes CCDC reference numbers 1841392 (MOF **2**) and 1841391 (MOF **3**).

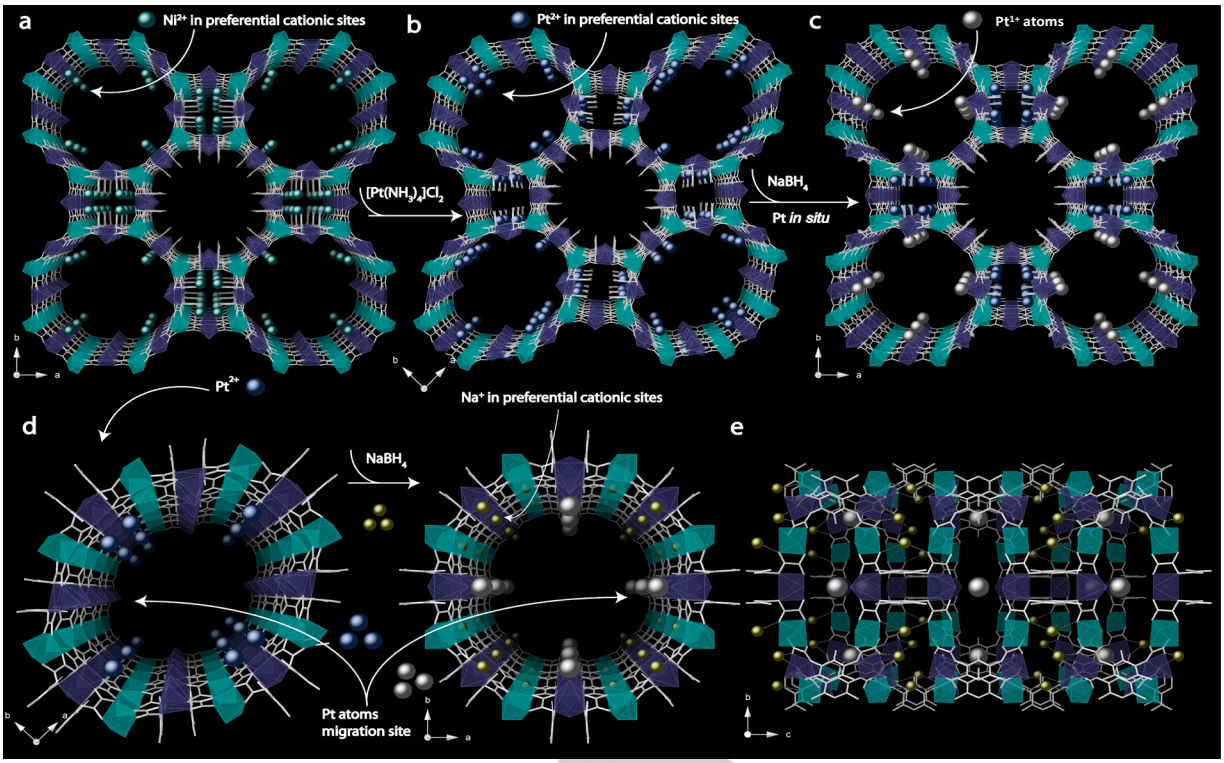

Figure 1. Experimental crystal structures of MOFs **1**–**3** (a-c), and perspective views along different axes (d-e) for **2** and **3**, respectively, showing in detail the Pt^{2+} (**2**) and the Na^+ and Pt_1^{1+} (**3**) sites. Cu and Ni atoms from the network are represented by cyan and purple polyhedra, respectively, whereas organic ligands are depicted as sticks. Green, blue, grey and yellow spheres represent Ni^{2+}, Pt^{2+}, Pt^{1+} and Na^+ atoms, respectively.

MOF **2** crystallizes in the *Cmmm* space groups of the orthorhombic system, with the Pt^{2+} cations located in the preferential sites of the hydrophilic octagonal pores [virtual diameter of 2.2 nm] previously occupied by the Ni^{2+} cations of **1**. Robustness together with flexibility of the net acts in response to Pt^{2+} exchange merely with a distortion of the pores' shape, accounting for a phase transition from a tetragonal to orthorhombic system (Figures S1–5, see also Table S2). Pt^{2+} moieties retain either the mononuclear nature as $[Pt(NH_3)_4]^{2+}$ (disordered on two positions, Figures S6 and S7) [average Pt^{2+}–N bond lengths of 1.995(9) Å] or they dimerize to give complexes likely of the type $[Pt_2(\mu\text{–}O)(NH_3)_6]^{2+}$ (some NH_3 molecules were not found from ΔF map in Figures S5–S7). In contrast, the crystal structure of **3** in Figure 1c reveals the formation of Pt_1^{1+} single metal cations confined into the, no longer distorted, hydrophilic octagonal channels of the *P*$_4$/*mmm* tetragonal anionic $Ni_4^{2+}Cu_6^{2+}$ open–framework net (Figures S3b, S4a, S5c–d and S8, and Table S2), together with unchanged $Pt^{2+}\cdots Pt^{2+}$ dimers in square pores and hydrated charge–counterbalancing alkali Na^+ cations in the preferential cationic sites. The worse accessibility to the square pores for solvated $NaBH_4$ is most likely at the origin of $Pt^{2+}\cdots Pt^{2+}$ intradimers not been reduced in **3**, as assessed by the persistence of the Pt^{2+}–NH_3 bands in FT–infrared spectroscopy (IR, Figure S5). Powder X–ray diffraction (PXRD) patterns (Figures S8–9) and N_2 adsorption isotherms at 77 K (Figure S10) for **2** and **3** are similar after the PS treatment, with calculated Brunauer–Emmett–Teller (BET) surface areas of 1142–1170 $m^2 \cdot g^{-1}$, which confirm that the porous structures are not affected either by the replacement of Ni^{2+} by Pt^{2+} cations or after $NaBH_4$ reduction. Quantitative X–ray photoelectron spectroscopy (XPS) of **2** and **3** (Figure S11) shows that half of the Pt^{2+} atoms in **3** (73.7 eV) have been reduced to a low–valence oxidation state after treatment with $NaBH_4$ (72.2 eV), and this value fits better that of unsaturated $Pt^{\delta+}$ species confined in MOFs[6] or ligated to thiols,[7] which corresponds to formal Pt^{1+} rather than to any typical signal for Pt(0) (<72.0 eV).[8] X–ray absorption near–edge structure (XANES) analysis of **3** (Figure S12) shows a discretely higher intensity for Pt in **3** respect to Pt foil, which indicates that the reduced Pt atoms are slightly oxidized.[9] The local environment around the Pt atom is also significantly different to Pt foil (see inset), with a flattening of the oscillations in the fine structure denoting discrete Pt entities.[10] Extended X–ray absorption fine structure (EXAFS) of **3** (Figures S13 and S14) shows a clear contribution around 1.7 Å, which corresponds to Pt–O or Pt–N bonds (notice the similar position of the first shell of PtO_2, not phase corrected), while the imaginary part of |FT| (Fourier transformation) early shifts to higher R values and, at certain point (ca. 2.4 Å), in antiphase respect to Pt foil. The absence of higher shells beyond 3 Å indicates that $Pt^{\delta+}$ atoms are highly dispersed within the structure of **3**.

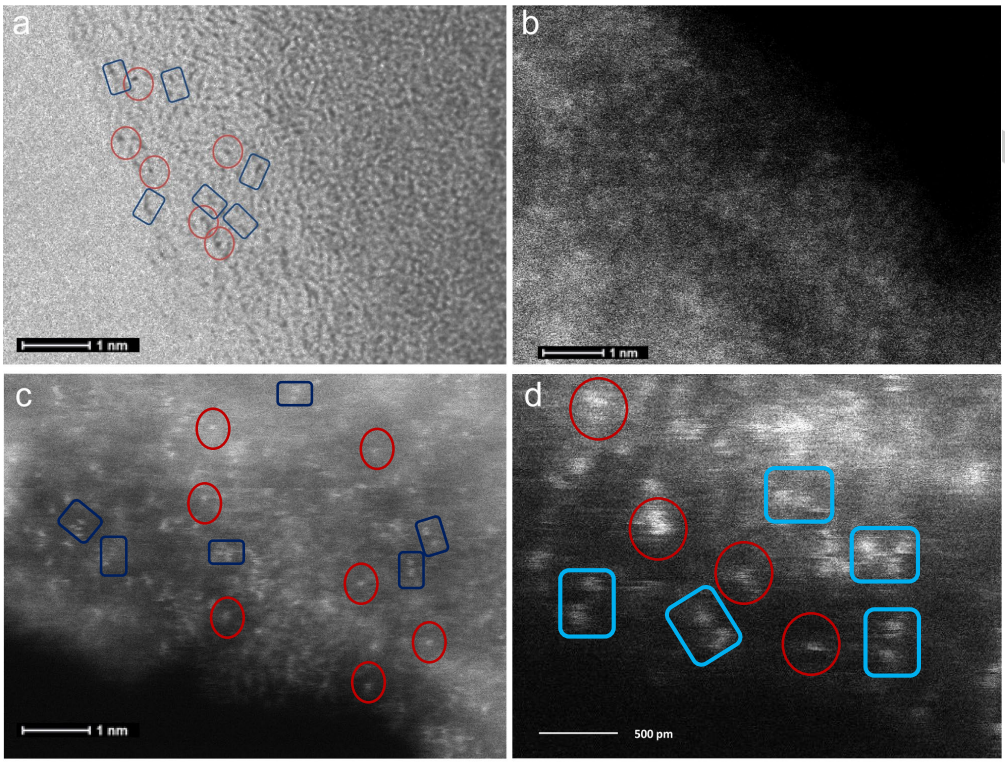

Figure 2. AC–HRTEM (a) and AC–HAADF–STEM (b) images of fresh **3**, where a homogenous distribution of Pt_1^{1+} atoms (circled in red) and $Pt^{2+}\cdots Pt^{2+}$ dimers (squared in blue) can be seen; c, d) AC–HAADF–STEM images of **3** recovered after the WGSR in flow for 4 hours at 150 ºC.

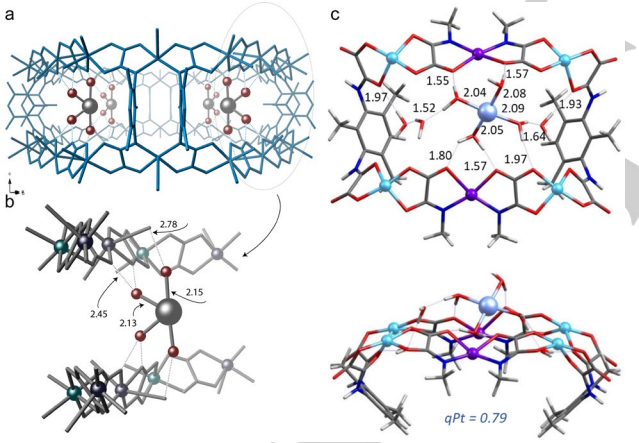

Figure 3. a, b) Detailed SC–XRD results of the Pt_1^{1+} complex within the MOF **3**. Colour scheme: Pt_1^{1+}, grey spheres; water oxygens, red spheres; Ni^{2+}, green spheres; Cu^{2+}, violet spheres; Pt metal atoms, not belonging to the net, have been omitted for clarity; carbon, oxygen and nitrogen ligands' atoms of the whole net have been depicted as sticks. Dotted lines correspond to hydrogen bonds. c) DFT optimized structure of the Pt_1^{1+} complex with seven water molecules. Colour scheme: Pt_1^{1+}, grey–blue sphere; oxygen atoms in red, hydrogen atoms in white, carbon atoms in grey; Ni^{2+}, green spheres; Cu^{2+}, violet spheres.

Figure 2 shows the aberration–corrected scanning transmission electron microscopy (AC–STEM, *Z*–contrast imaging, Figure 2a) and high–angle annular dark field (HAADF, Figure 2b) images of **3**, where the original $Pt^{2+}\cdots Pt^{2+}$ dimers together with Pt_1^{1+} species are clearly observed, thus confirming the lack of aggregation of Pt inside the MOF.

Figures 3a–b shows the detailed structure of the Pt_1^{1+} complex in the MOF according to SC–XRD. It can be seen that the Pt_1^{1+} atom is well fixed in the large pores by a net of coordinated water molecules [Pt– O_{water} average distance of 2.14(1) Å] and stabilized by very strong bifurcated (2.45(1) Å) and moderate (2.78(1) Å) hydrogen bonds, involving the oxygen atoms of the oxamate ligands and apical water molecules of the Jahn–Teller distorted Cu^{2+} of the net (see also Figures S4 and S14).

Figure 3c shows the DFT optimized structure of Pt_1^{1+} in **3** and confirms the feasibility of the experimental XRD structure found, with four water molecules directly attached to Pt at a Pt–O_{water} average distance of 2.06 Å, and three more water molecules in the second coordination sphere, linked to the $Pt_1^{1+}(H_2O)_4$ unit and the MOF ligands by strong hydrogen bonds. These results illustrate the stabilization provided by the nano–confined space of the MOF not only with a primary but also with a second water coordination sphere. Analysis of the charge distribution gives a charge for the Pt atom of +0.8, which nicely fits the electroneutral formula for **3** (see above) found by inductively coupled plasm–mass spectrometry (ICP–MS) and elemental analysis, and that corresponds to an equimolar Pt^{1+}:Pt^{2+} ratio. With these results at hand, and considering the rest of experimental techniques (see also Figure S15), we can say that a Pt_1^{1+} single site just stabilized by water molecules within the MOF structure, has been obtained in gram–scale.

The water–gas shift reaction WGSR (CO + H_2O → CO_2 + H_2) is an industrial reaction that provides an easy source of H_2 from the surplus CO generated by other processes.[11] Highly promising fuel cell technologies rely on the WGSR[12] as long as new catalysts, operating at temperatures <150 ºC and compatible with fuel cell applications, are developed. In this context, several works have reported that Pt_1 and Au_1 with a certain positive charge, anchored on solids through strong metal–support interactions (SMSI) or modified with alkali precursors, efficiently catalyze the WGSR at temperatures compatible with fuel cells.[13–14] However, in the case of Pt, the exact catalytic active species is still under debate, since Pt nanoparticles (NPs) and not Pt_1 have been explicitly claimed as the only active species of the low–temperature WGSR, regardless the support.[15]

Water adsorption isotherms of the activated compounds **2** and **3** at 50 ºC show a similar large water uptake and a complete rehydration, consisting of the recovery of 26 and 29 mmol of water per gram of MOF (Figure S16), in agreement with TGA analyses (Figure S17). However, the CO adsorption isotherms are different for **2** and **3**. The CO uptake is higher for **2** but irreversible (Figure S18), which contrasts with the reversible adsorption isotherm for **3**. CO FT–IR shows that CO adsorbs at -178 ºC on the available Pt^+ sites of **2** (Pt^{2+}) and **3** (Pt^{1+}) with different intensity (Figure S19), and that Pt^{1+}–CO signals in **3** disappear when heating to give CO_2 as a product, while any adventitious Pt(0) species do not react.[16] These results indicate that CO adsorbs very weakly on aqueous Pt_1^{1+} and that, at near room temperature, gives CO_2, which makes **3** a potentially powerful catalyst for the WGSR, since the catalytic activity of Pt for this reaction is related to its ability to co–adsorb water and CO without CO poisoning.[15] While it is true that Figure S19 also indicates that some Pt^0 can be present or formed during reaction conditions, all the data shown above soundly point to the major Pt species in the MOF, i.e. Pt^{1+}, as the only responsible for the catalytic activity.

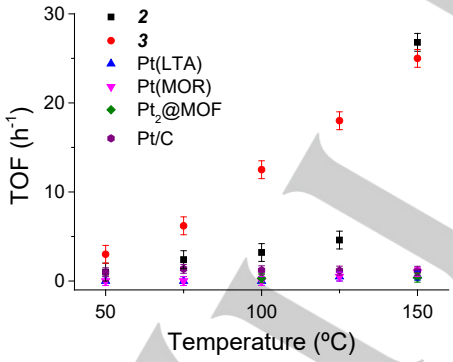

Figure 4. Temperature–programmed WGSR catalyzed by **3** and other Pt–supported catalysts in–flow.

Figure 4 shows the catalytic results for **2**, **3**, and other Pt–supported catalysts for the low–temperature WGSR in flow(weight hourly spatial velocity, WHSV= 60 000 ml g_{cat}^{-1} h^{-1}). MOF **3** catalyzes the reaction from 50 to 200 ºC with a steady increase in TOF (calculated as mol of CO_2 per mol of Pt_1^{1+} and hour) from 5 to 108 h^{-1}. In contrast, the rest of Pt–supported catalysts tested, which includes Pt on carbon, Pt reduced in the small pores (ca. 0.8 nm) of zeolite KLTA[17] and mordenite (MOR), a related MOF structure with Pt^0 dimers,[18] and MOF **2**, showed small (TOF <5 h^{-1}) or no activity up to 150 ºC. The abrupt increase in catalytic activity of MOF **2** can tentatively be assigned to autoreduction of Pt^{2+}. Previous low–temperature WGSR Pt catalysts have not shown any catalytic activity below 100 ºC[13,15] and, accordingly, the calculated activation energy for **3** is 5 Kcal lower (12 Kcal mol^{-1}) than previous Pt catalysts, while the TOF obtained at 200 ºC is similar (0.03 s^{-1}).[13] These results indicate that Pt_1^{1+} is a very active SAC for the low–temperature WGSR, while the Pt^{2+} species in **2** or **3** are not active at temperatures below 150 ºC.

PXRD patterns of **3** recovered after 4 hours on the WGSR stream at 150 ºC (Figure S9) show the retention of crystallinity and porosity of the used material, and does not show any characteristic XRD peaks of Pt NPs or metal oxide crystals. AC–HAADF–STEM images of the same sample (Figures 2c–d above), in combination with XPS measurements (Figure S11), confirm the stability of the Pt_1^{1+} SAC sites after reaction, which remain homogeneously distributed along the MOF. A 0.5 nm resolved image (Figure 2d) shows the persistence and good distribution of the Pt sites on **3** after reaction. Treatment of **3** in the XPS chamber with either CO, H_2O vapor or H_2 does not produce significant modifications of the original Pt spectrum, with equimolecular amounts of low–valence Pt_1^{1+} and $Pt^{2+}\cdots Pt^{2+}$ dimers still present. The H_2O molecules in the first and second coordination spheres persist bound to Pt_1^{1+} during reaction, as assessed by comparison of the FT–IR spectrum of **3** with samples treated with D_2O or $H_2{}^{18}O$ during 3 h at 150 ºC and then evacuated under vacuum (Figure S20). These results illustrate the robustness of Pt_1^{1+} stabilized by water clusters within the MOF during reaction.

The WGSR with labelled $H_2{}^{18}O$ as reagent, in batch, forms mainly $C^{18}O_2$ when catalyzed by **3** (Table S3–4 and Figure S21). This striking result can only be explained by the incorporation of two water molecules in the final CO_2 product. One is tempted to think that a scrambling of the CO and water oxygen atom occurs. However, GC–MS shows <1% of isotopically labelled $C^{18}O$ in the reaction atmosphere. Indeed, kinetics with 10 times excess of CO respect to $H_2{}^{18}O$ show that $C^{18}O_2$ and regular H_2O are still formed from the very beginning of the reaction, and as the reaction progresses, regular CO_2 and mixed $CO^{18}O$ are formed statistically, depending on the ratio H_2O/H_2O^{18} in the media. The final mixture contains >50% of isotopically labelled $C^{18}O_2$, a much higher proportion than expected for a thermodynamic mixture at these reaction conditions (isotopic molar ratio CO_2: $CO^{18}O$: $C^{18}O_2$ 10:6:1) and more similar to a reaction going through a long–lived formate or orthoformate intermediate (1:3:5, Figure S22). ^{13}C magic angle spinning solid nuclear magnetic resonance (MAS NMR) of ^{13}CO co–adsorbed with water on **3** ($CO:H_2O$ 1:2 equivalents respect to Pt) into a sealed rotor and heated at increasing temperatures, shows the progressive disappearance of the ^{13}CO signal at expenses of a new signal at 156 ppm, which progressively transforms into $^{13}CO_2$ when heating (Figure S23). The signal at 156 ppm also appears in cross–polarization NMR, which indicates that the ^{13}C atom has H atoms at 1–2 bond distance, and the NMR value fits that expected for an intermediate orthoformate. These results indicate that H_2O attacks twice to CO to form the intermediate orthoformate, which would collapse into CO_2 after scrambling the oxygen atoms of CO and H_2O (Figure S24).

The experimental kinetic rate equation found for **3** is $v_0=k_{app}[CO][\mathbf{3}]$ for >0.1 equivalents of water and $v_0=k_{app}[CO][H_2O][\mathbf{3}]$ for lower water amounts, and no kinetic isotopic effect (KIE, ≈1.0) occurs when using D_2O as reactant.

These results support that the adsorption and coupling of CO in the H_2O saturated Pt_1^{1+} site is the rate–determining step (rds) of the reaction (Table S5) and that coordinated H_2O molecules act catalytically during the reaction. The state–of–the–art SAC Pt_1–Na/SiO_2[13] were prepared by us and tested in the WGSR in batch, showing the same isotopic distribution than **3** when $H_2{}^{18}O$ was used as reactant, with $C^{18}O_2$ again as the major product (Table S3), and also the same form of rate equation (Figure S25). The less active SAC Pt_1/SiO_2[11] was also prepared and the results obtained were consistent (Tables S6–7). These results, suggest that the "waterborne" CO_2 oxygen atom mechanism is somewhat general for other Pt catalysts and not particular for **3**.

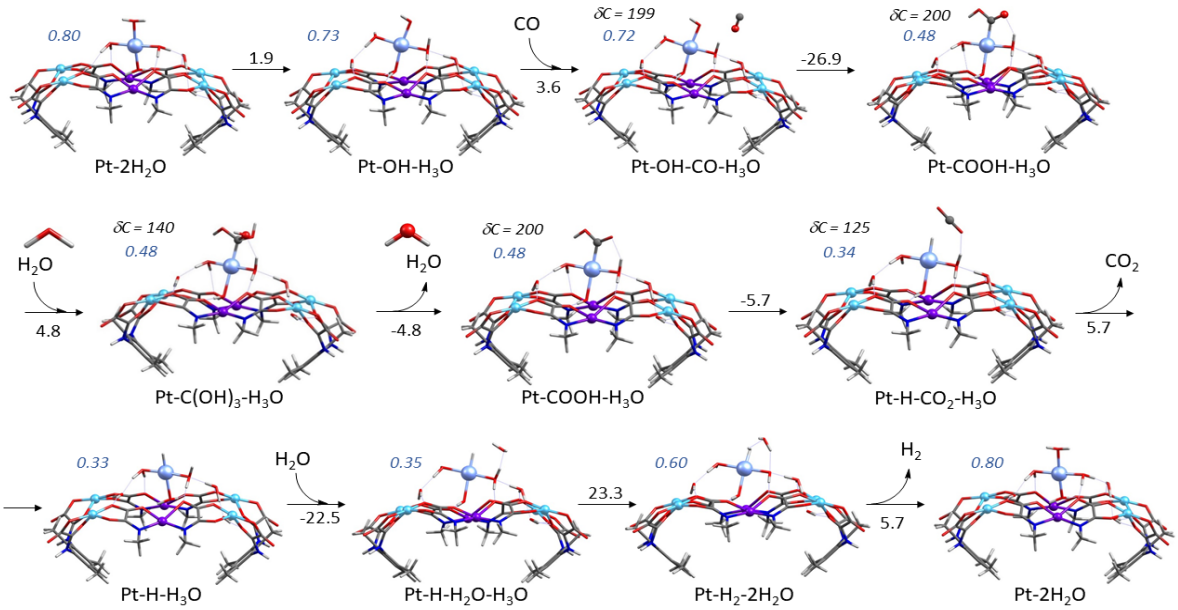

Figure 5. Plausible mechanism of the low–temperature WGSR catalyzed by the Pt_1^{1+} water cluster in **3** as indicated by the experimental results and DFT calculations. Numbers in blue correspond to Pt_1 net charge. Black numbers on/below the arrows are the Gibbs free energies ΔG^o for each elementary step, in Kcal mol^{-1}. δC is the calculated NMR shift of the carbon atom. Colour scheme: Pt_1^{1+}, grey–blue sphere; oxygen atoms in red, hydrogen atoms in white, carbon atoms in grey; Cu^{2+}, violet spheres; Ni^{2+}, light blue spheres.

Figure 5 shows the possible mechanism for the low–temperature WGSR on the Pt_1^{1+} single site stabilized by water clusters, supported by DFT calculations. The more reactive coordinated H_2O molecule, away from the MOF walls, transfers a proton first to a neighbor H_2O directly attached to Pt_1^{1+} and then to another H_2O in the second coordination sphere, to give an –OH group on Pt_1^{1+} and a H_3O^+ cation on the water cluster (Figure S26). This OH, and not H_2O, assists CO to be activated on Pt_1, which is the rds of the reaction. The activated CO undergoes first the addition of OH and then H_2O, to give the intermediate orthoformate Pt–$C(OH)_3$ in equilibrium with the formate Pt–COOH.[14b] The latter transfers the hydrogen atom to Pt_1^{1+} via *beta* elimination, which then releases CO_2 and H_2 after the water–assisted reaction of the hydride (Figure S27). Notice that the calculated ^{13}C NMR value (δC) for the orthoformate intermediate fits well with the signal detected experimentally, much more than any other species. The network of water molecules surrounding the Pt_1^{1+} site are continuously regenerated by the external water during reaction and prevents saturation and catalyst deactivation by CO, and also stabilizes a proton in the catalytic site to form H_2 and re–start a new catalytic cycle.

In summary, Pt_1^{1+} coordinated and stabilized by a water cluster in a MOF can be obtained in gram–scale and used as an efficent catalyst for the low–temperature WGSR and a double water attack mechanism to give CO_2, where both oxygen atoms come from water. These results open new avenues in the design of SACs[19] and expand the understanding of the low–temperature WGSR mechanism.

Acknowledgements

This work was supported by the MINECO (Spain) (Projects CTQ2016–75671–P, MAT2013 40823–R, MAT2016–81732–ERC, CTQ2017–86735–P, MAT2017–86992–R, MAT2017–82288–C2–1–P and Excellence Units "Severo Ochoa" and "Maria de Maeztu" SEV–2016–0683 and MDM–2015–0538) the Generalitat Valenciana (PROMETEOII/2014/004) and the Ministero dell'Istruzione, dell'Università e della Ricerca (Italy) and the Junta de Andalucía (FQM–195). M. M. and M.–A. R. C. thanks the MINECO for a predoctoral contract. Thanks are also extended to the Ramón y Cajal Program (E. V. R.–F., E. P. and J.–C. H.–G.) and the "Subprograma atracció de talent–contractes postdoctorals de la Universitat de Valencia" (J. F.–S.). M. L.–H. acknowledges the financial support from the Juan de la Cierva Fellowships Program of MINECO (IJCI–2014–19367).

Keywords: single atom catalyst • metal-organic frameworks • platinum • water clusters • water–gas shift reaction

[1] a) M. Flytzani–Stephanopoulos, B. C. Gates, *Annu. Rev. Chem. Biomol. Eng.* **2012**, *3*, 545–574.; b) L. Liu, A. Corma, *Chem. Rev.* **2018**, *118*, 4981–5079.

[2] a) O. K. Farha, J. T. Hupp, *Acc. Chem. Res.* **2010**, *43*, 1166–1175; b) H. Furukawa, K. E. Cordova, M. O'Keeffe, O. M. Yaghi, *Science* **2013**, *341*, 974.

[3] a) F. R. Fortea-Pérez, M. Mon, J. Ferrando-Soria, M. Boronat, A. Leyva-Pérez, A. Corma, J. M. Herrera, D. Osadchii, J. Gascon, D. Armentano, et al., *Nat. Mater.* **2017**, *16*, 760–766; b) H. Liu, L. Chang, C. Bai, L. Chen, R. Luque, Y. Li, *Angew. Chem. Int. Ed.* **2016**, *55*, 5019–5023.

[4] S. M. Cohen, *J. Am. Chem. Soc.* **2017**, *139*, 2855–2863.

[5] T. Grancha, J. Ferrando–Soria, H–C Zhou, J. Gascon, B. Seoane, J. Pasán, O. Fabelo, M. Julve, E. Pardo. *Angew. Chem. Int. Ed.* **2015**, *54*, 6521–6525.

[6] R. Vakili, E. K. Gibson, S. Chansai, S. Xu, N. Al–Janabi, P. P. Wells, C. Hardacre, A. Walton, X. Fan. *ChemCatChem* **2018**, *10*, 4238–4242.

[7] X. Fu, Y. Wang, N. Wu, L. Gui, Y. Tang. *J. Col. Interf. Sc.* **2001**, *243*, 326–330.

[8] J. R. Reimers, M. J. Ford, A. Halder, J. Ulstrup, N. S. Hush. *Proceed. Nat. Am. Soc.* **2016**, *113*, 1424–1433.

[9] L. Liu, U. Díaz, R. Arenal, G. Agostini, P. Concepción, A. Corma, *Nat. Mater.* **2016**, *16*, 132–138.

[10] M. S. Nashner, A. I. Frenkel, D. L. Adler, J. R. Shapley, R. G. Nuzzo, *J. Am. Chem. Soc.* **1997**, *119*, 7760-7771.

[11] C. Ratnasamy, J. P. Wagner, *Catal. Rev.* **2009**, *51*, 325–440.

[12] W. Vielstich, A. Lamm, H. A. Gasteiger, H. Yokokawa, Eds., *Handbook of Fuel Cells* (John Wiley & Sons, Ltd, Chichester, UK, **2010**; http://doi.wiley.com/ 10.1002/ 9780470974001).

[13] a) Q. Fu, H. Saltsburg, M. Flytzani–Stephanopoulos, *Science* **2003**, *301*, ; b) Y. Zhai, D. Pierre, R. Si, W. Deng, P. Ferrin, A. U. Nilekar, G. Peng, J. A. Herron, D. C. Bell, H. Saltsburg, M. Mavrikakis, M. Flytzani–Stephanopoulos, *Science* **2010**, *329*, 1633–1636.

[14] a) J. A. Rodriguez, P. J. Ramírez, G. G. Asara, F. Viñes, J. Evans, P. Liu, J. M. Ricart, F. Illas, *Angew. Chemie Int. Ed.* **2014**, *53*, 11270–11274; b) S. Yao, X. Zhang, W. Zhou, R. Gao, W. Xu, Y. Ye, L. Lin, X. Wen, P. Liu, B. Chen, E. Crumlin, J. Guo, Z. Zuo, W. Li, J. Xie, L. Lu, C. J. Kiely, L. Gu, C. Shi, J. A. Rodriguez, D. Ma, *Science* **2017**, *357*, 389–393.

[15] K. Ding, A. Gulec, A. M. Johnson, N. M. Schweitzer, G. D. Stucky, L. D. Marks, P. C. Stair, *Science* **2015**, *350*, 189–192.

[16] a) L. Drozdova, L. Kubelkova, *J. Chem. Soc., Faraday Trans.* **1997**, *93*, 2597–2602; b) A. Garnier, S. Sall, F. Garin, M. J. Chetcuti, C. Petit, *J. Mol. Catal. A* **2013,** *373*, 127–134.

[17] J. D. Kistler, N. Chotigkrai, P. Xu, B. Enderle, P. Praserthdam, C. –Y. Chen, N. D. Browning, B. C. Gates, *Angew. Chem. Int. Ed.* **2014**, *53*, 8904–8907.

[18] M. Mon, M. A. Rivero–Crespo, J. Ferrando–Soria, A. Vidal–Moya, M. Boronat, A. Leyva–Pérez, A. Corma, J. C. Hernández–Garrido, M. López–Haro, J. J. Calvino, G. Ragazzon, A. Credi, D. Armentano, E. Pardo, *Angew. Chem., Int. Ed.* **2018**, *57*, 6186–6191.

[19] a) X. Cui, K. Junge, X. Dai, C. Kreyenschulte, M.-M. Pohl, S. Wohlrab, F. Shi, A. Brückner, M. Beller, *ACS Cent. Sci.* **2017**, *3*, 580–585, b) K.–i. Otake, Y. Cui, C. T. Buru, Z. Li, J. T. Hupp, O. K. Farha, *J. Am. Chem. Soc.* **2018**, *140*, 8652−8656.

10.1002/anie.201810251

WILEY-VCH

Entry for the Table of Contents

COMMUNICATION

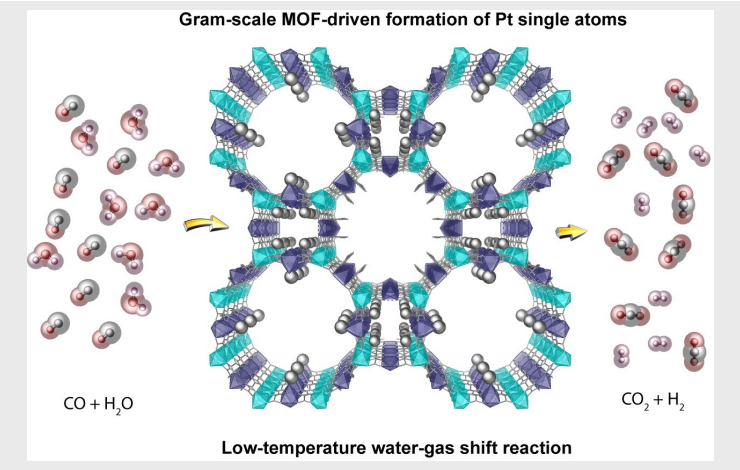

A catalyst with Pt_1^{1+} exclusively coordinated to H_2O molecules can be prepared in gram–scale within a MOF to transfer two H_2O molecules to CO and give, very efficiently, CO_2 and H_2 (water–gas shift reaction) at 50–150 ºC.

Miguel A. Rivero–Crespo, Marta Mon Jesús Ferrando–Soria, Christian W. Lopes, Mercedes Boronat, Antonio Leyva–Pérez, Avelino Corma,* Juan C. Hernández–Garrido, Miguel López–Haro, Jose J. Calvino, Enrique V. Ramos–Fernandez, Donatella Armentano* and Emilio Pardo.**

Page No. – Page No.

Confined Pt_1^{1+}–water clusters in a MOF Catalyze the Low–Temperature Water–Gas Shift Reaction with both CO_2 Oxygen Atoms Coming from Water.